Published in final edited form as:
Opt Lett. 2012 March 1; 37(5): 981–983.

Optical detection of indocyanine green encapsulated biocompatible poly (lactic-co-glycolic) acid nanoparticles with photothermal optical coherence tomography

Hrebesh M. Subhash[1,2,*], **Hui Xie**[3], **Jeffrey W. Smith**[3], and **Owen J. T. McCarty**[1]

[1]Department of Biomedical Engineering, Oregon Health and Science University, 3303 SW Bond Ave., Portland, Oregon 97239, USA

[2]Oregon Hearing Research Center, School of Medicine, Oregon Health and Science University, 3181 SW Sam Jackson Park Road, Portland, Oregon 97239, USA

[3]Program for Excellence in Nanotechnology, Sanford-Burnham Medical Research Institute, La Jolla, California 92037, USA

Abstract

We describe a functional imaging paradigm that uses photothermal optical coherence tomography (PT-OCT) to detect indocyanine green (ICG)-encapsulated biocompatible poly(lactic-co-glycolic) acid (PLGA) nanoparticles embedded in highly scattering tissue phantoms with high resolution and sensitivity. The ICG-loaded PLGA nanoparticles were fabricated using a modified emulsification solvent diffusion method. With a 20 kHz axial scan rate, PT-OCT based on spectral-domain interferometric configuration at 1310 nm was used to detect phase changes induced by a 808 nm photothermal excitation of ICG-encapsulated PLGA nanoparticles. An algorithm based on Fourier transform analysis of differential phase of the spectral interferogram was developed for detecting the depth resolved localized photothermal signal. Excellent contrast difference was observed with PT-OCT between phantoms containing different concentrations of ICG-encapsulated PLGA nanoparticles. This technique has the potential to provide simultaneous structural and molecular-targeted imaging with excellent signal-to-noise for various clinical applications.

In the rapidly evolving field of biomedical imaging, optical coherence tomography (OCT) [1] is one of the most promising optical methods for noninvasive volumetric imaging and characterization of biological tissues with high resolution and sensitivity. OCT has several advantages over other clinical imaging technologies, as OCT enables real-time, *in situ* and *in vivo* visualization of tissue microstructures with image resolution scales approaching those of histopathology. However, as OCT relies on detecting the coherence scattering from the refractive index boundaries of tissue microstructures, OCT imaging provides only limited molecular information of clinically relevant structures. This is due to the fact that OCT is intrinsically insensitive to incoherent scattering phenomenon such as fluorescence and spontaneous Raman scattering, which are the key to molecular imaging. Thus, there is a great interest in enhancing the utility of OCT for molecular imaging through the incorporation of extrinsic contrast agents such as iron oxide particles, proteins, dyes and various types of gold nanoparticles [2–4]. Among them, gold nanoparticles have shown more promise as contrast agents for diagnostic imaging via OCT, due to their plasmon resonance or near-IR absorbing properties [5–8]. However, when choosing a nanoparticulate

*Corresponding author: mollysub@ohsu.edu.

system for the development of contrast imaging agents, the toxicology, clearance, and metabolite profile of these nanoparticles must be carefully considered [9–11]. The pharmacokinetic and safety profile of gold nanoparticles and other metal-based nanoparticles has yet to be sufficiently defined [12–13]. Thus the use of biocompatible and biodegradable contrast carriers with well-defined toxicological profiles, clearance, and safety profiles, such as poly(lactic-co-glycolic) acid (PLGA) (approved by the U.S. Food and Drug Administration), are ideal for clinical utility [14–15]. Near-IR, polymeric, biodegradable/biocompatible nanoparticles belong to a new class of multifunctional biophotonic agents for diagnostic and treatment applications. In this study, we report the first experimental demonstration of the feasibility of imaging dye-loaded PLGA nanoparticles using photothermal OCT (PT-OCT).

Indocyanine green (ICG) is a water soluble tricarbocyanine dye approved by the FDA for a number of applications [16]. ICG-loaded PLGA nanoparticles were prepared by a modified spontaneous emulsification solvent diffusion method. A scanning electron microscope (SEM) was used to determine the particle size, which was ~367 ± 80 nm. At the current stage of development, we did not attempt to strictly control the nanoparticle size distribution or ICG encapsulation efficiency. The peek absorption of the particles were observed at 810 nm.

A PT-OCT system based on spectral-domain interferometric configuration with an axial scan rate of 20 KHz was developed for these studies. Figure 1 illustrates the schematic of the PT-OCT system. The light from a 56 nm bandwidth low-coherence broadband infrared superluminescent diode light (SLD) source (1300 ± 28 nm) was coupled into a 10:90 fiber based Michelson interferometer, via an optical coupler. This spectrometer setup had a spectral resolution of 0.155 nm, which gave a maximum imaging depth of ~2.15 mm (in phantom). The measured axial resolution of the PT-OCT system was around 15 μm in air. A fiber coupled pump laser with an output power of 80 mW was used for photothermal excitation. The peek wavelength of the laser was around 808 nm, which was very close to the absorption peek of the ICG-encapsulated PLGA nanoparticles. At the sample arm, the pump laser output (808 nm) was collinearly coupled to the imaging beam (1310 nm) using a diachronic mirror, as shown in Fig. 1. The collinearly coupled sample beam and excitation beam were delivered into the sample using a 50 mm achromatic lens. The focal spot size of the excitation laser was measured with a CCD camera, which was around 170 μm and the spot size of the imaging beam was ~25 μm, as estimated with a USAF 1951 test target.

The pump laser was modulated by a digital pulse generator and was synchronized with the camera. The phase sensitivity of the system was estimated to be around 7.5 mrad, corresponding to a displacement sensitivity of 785 picometers. PT-OCT configuration based on common-path interferometers [5–7] can provide a displacement sensitivity of the order of tens of picometers. In order to compute the cross-sectional PT-OCT images, a MB-scan mode scanning protocol was implemented. In the transverse direction of the images, a 1000-line M-mode acquisition was performed at each transverse position with an A-scan rate of 5307 Hz. During acquisition, the sample was excited using the photothermal excitation laser with a square wave modulation frequency of 1000 Hz. Photothermal excitation radiation was absorbed by the ICG-encapsulated PLGA nanoparticles, which induced localized heating of the particles. Subsequent dissipation of heat from the nanoparticles into the surrounding tissue phantoms created a temperature distribution, which in turn produced a small shift in refractive index of the surrounding tissue phantoms. This change in localized refractive index caused changes in the optical path length within the imaging tissue phantom, corresponding to the photothermal signal. These photothermal signals were encoded in the phase of the spectral interferogram.

To extract the photothermal signal, a custom processing algorithm was used to analyze the BM-mode OCT data. The phase was then calculated for each corresponding pixel of the M-mode image, and the phase difference between adjacent A-lines was computed, which was proportional to modulation of the optical path difference induced by the excitation laser. The phase difference between adjacent A-scans, j and $j-1$, can be calculated as

$$\Delta\Phi(z,t)=\arctan(\mathrm{Im}[I(z,t_j)I^*(z,t_{j-1})]/\mathrm{Re}[I(z,t_j)I^*(z,t_{j-1})]), \quad (1)$$

where * denotes the complex conjugate. Then the Fourier transformations of this measured phase differences, i.e., Eq. (1) can be taken as $p(z, f) = \mathrm{FT}[\Delta\Phi(z, t)] = |p(f)| \exp[i\theta(f)]$, where f is the frequency variable of interest for the photothermal signal, and $p(f)$ and $\theta(f)$ are the magnitude and phase of the signal at frequency f. Thus peak magnitude of fast Fourier transform (FFT) within ±10 Hz of the modulation frequency (1 KHz) was taken for each M-mode OCT dataset and was used to obtain a 2D depth resolved cross-sectional photothermal OCT image.

To demonstrate the concept of photothermal detection of ICG-encapsulated PLGA nanoparticles with PT-OCT, five increasing concentrations of ICG-encapsulated PLGA nanoparticles, ranging from 0–10 mg/ml, were embedded into a tissue phantom. The tissue phantom was fabricated with a 2% agarose solution (99.99%, Sigma-Aldrich) and polystyrene microspheres concentration of 0.191 spheres/μm^3. Based on Mie theory, this concentration yielded a scattering coefficient of 84.69 mm^{-1} for the phantoms alone, which is very similar to the scattering coefficient of biological tissue. The photothermal signal was extracted by the signal processing steps described above. Figure 2(a) shows the FFT amplitude of the differential phase of the spectral interferogram calculated for the tissue phantom at a particular depth with a particle concentration of 7.5 mg/ml. The FFT amplitude was calibrated to the corresponding optical path displacement. Next, we measured the maximum optical path displacement for tissue phantoms embedded with ICG-encapsulated PLGA nanoparticles with a photothermal modulation frequency of 1 KHz. Figure 2(b) shows the plot of maximum optical displacement amplitude obtained with increasing concentrations of nanoparticles. To compute 2D depth resolved cross-sectional PT-OCT images, we made four cylindrically shaped tissue phantoms with nanoparticle concentrations of 0 mg/ml, 2.5 mg/ml, 5 mg/ml, and 10 mg/ml. The samples were stacked together and an MB-mode scan was performed along the transverse direction at 600 transverse points with a scan range of 5 mm. Within each step, the data acquisition time was ~200 ms and it requires ~120 sec to scan to 600 steps across the sample. Figure 3(a) shows the structural image obtained using the conventional spectral-domain OCT, and Fig. 3(b) shows the corresponding PT-OCT image obtained by the photothermal excitation of the tissue phantom. Our data show that the PT-OCT image of the tissue phantom clearly reveals the concentration of the dye-loaded PLGA nanoparticles embedded in the tissue with high signal contrast.

In conclusion, we have demonstrated the optical detection of ICG-encapsulated PLGA nanoparticles with PT-OCT. The technical feasibility of depth resolved functional imaging was demonstrated with tissue phantoms embedded with different particle concentrations. Since ICG and PLGA are both FDA approved biocompatible materials, the ICG-encapsulated PLGA nanoparticles may introduce fewer clinical safety concerns in comparison with other metal-based nanoparticles, such as gold and its derivatives. Moreover, detection sensitivity could be increased by developing nanoparticles with higher encapsulation efficiency, resulting in increased photothermal contrast with low power excitation levels and/or particle concentration. PLGA and its various derivates are well

developed for functional targeting applications, and in the future we aim to enhance the capability of these nanoparticles for selective targeting.

Acknowledgments

This work was supported by National Institutes of Health (NIH) grants R01HL101972 and U54CA143906 (O.J.T.M.). The content is solely the responsibility of the authors and does not necessarily represent the official view of the NIH. The authors would like to thank Nina Chachi, MS, and Dan Jefferys-White, BA, for assisting in the preparation of tissue phantom and absorption spectroscopic studies.

References

1. Huang D, Swanson EA, Lin CP, Schuman JS, Stinson WG, Chang W, Hee MR, Flotte T, Gregory K, Puliafito CA, Fujimoto JG. Science. 1991; 254:1178. [PubMed: 1957169]
2. Oldenburg AL, Gunther JR, Boppart SA. Opt Lett. 2005; 30:747. [PubMed: 15832926]
3. Yang C, Choma MA, Lamb LE, Simon JD, Izatt JA. Opt Lett. 2004; 29:1396. [PubMed: 15233447]
4. Xu C, Ye J, Marks DL, Boppart SA. Opt Lett. 2004; 29:1647. [PubMed: 15309847]
5. Skala MC, Crow MJ, Wax A, Izatt JA. Nano Lett. 2008; 8:3461. [PubMed: 18767886]
6. Adler DC, Huang SW, Huber R, Fujimoto JG. Opt Express. 2008; 16:4376. [PubMed: 18542535]
7. Zhou C, Tsai TH, Adler DC, Lee HC, Cohen DW, Mondelblatt A, Wang Y, Connolly JL, Fujimoto JG. Opt Lett. 2010; 35:700. [PubMed: 20195324]
8. Jung Y, Reif R, Zeng Y, Wang RK. Nano Lett. 2011; 11:2938. [PubMed: 21667930]
9. Lewinski N, Colvin V, Drezek R. Small. 2008; 4:26. [PubMed: 18165959]
10. Murthy SK. Int J Nanomed. 2007; 2:129.
11. Wagner V, Dullaart A, Bock AK, Zweck A. Nat Biotechnol. 2006; 24:1211. [PubMed: 17033654]
12. Goodman CM, McCusker CD, Yilmaz T, Rotello VM. Bioconjugate Chemistry. 2004; 15:897. [PubMed: 15264879]
13. Pan Y, Neuss S, Leifert A, Fischler M, Wen F, Simon U. Small. 2007; 3:1941. [PubMed: 17963284]
14. Saxena V, Sadoqi M, Shao J. Int J Pharm. 2004; 278:293. [PubMed: 15196634]
15. Shah N, Chaudhari K, Dantuluri P, Murthy RS, Das S. J Drug Target. 2009; 17:533. [PubMed: 19530913]
16. Benson RC, Kues HA. Phys Med Biol. 1978; 23(1):159. [PubMed: 635011]

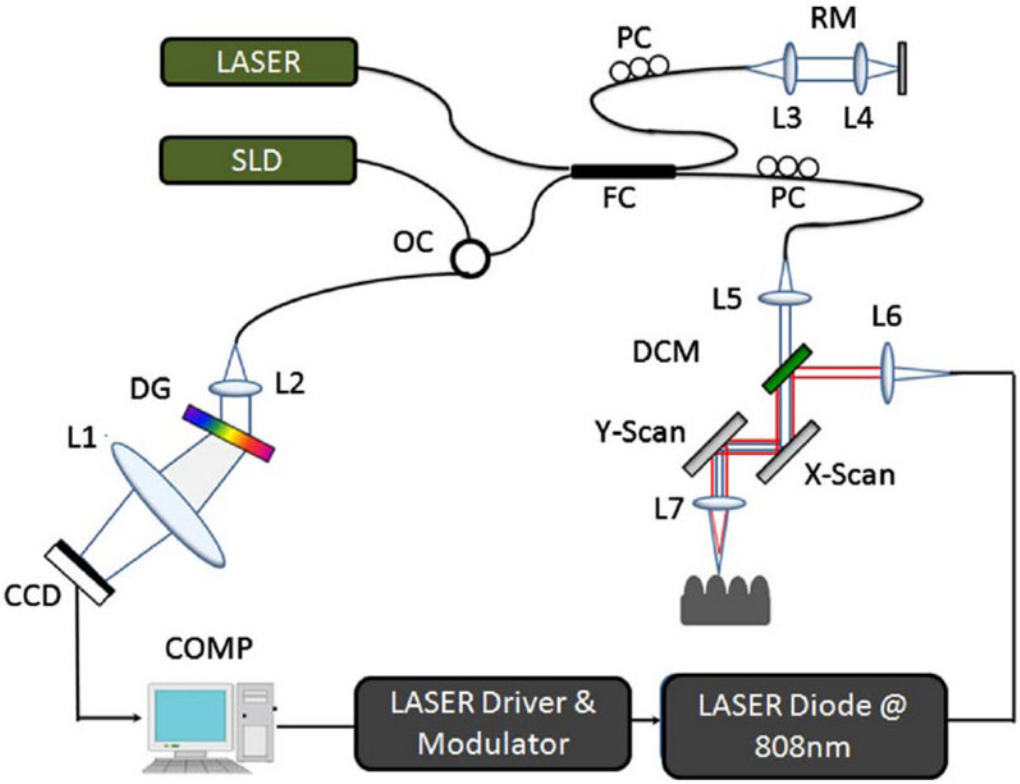

Fig. 1.

(Color online) Schematic of PT-OCT setup based on a spectral—domain interferometric configuration with photothermal modulation system. L1-L6, lenses. PC, polarization controller. FC, fiber coupler. DG, diffraction grating. OC, optical circulator. RM, reference mirror. SLD, superluminescent diode. DCM, diachronic mirror. COMP, computer.

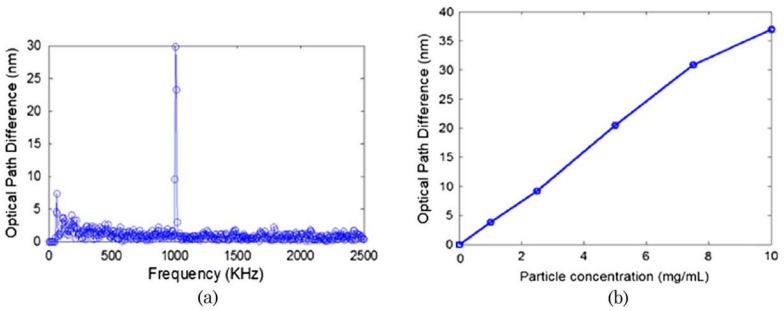

Fig. 2.

(Color online) Fourier transform of phase difference of M-scan spectral interferogram taken with ICG-encapsulated PLGA nanoparticles (7.5 mg/ml) at a particular depth inside the embedded tissue phantom with a modulation frequency of 1 KHz. (b) Optical path length change detected with PT-OCT for samples with five increasing concentrations (0 mg/ml, 2.5 mg/ml, 5 mg/ml, 7.5 mg/ml, and 10 mg/ml).

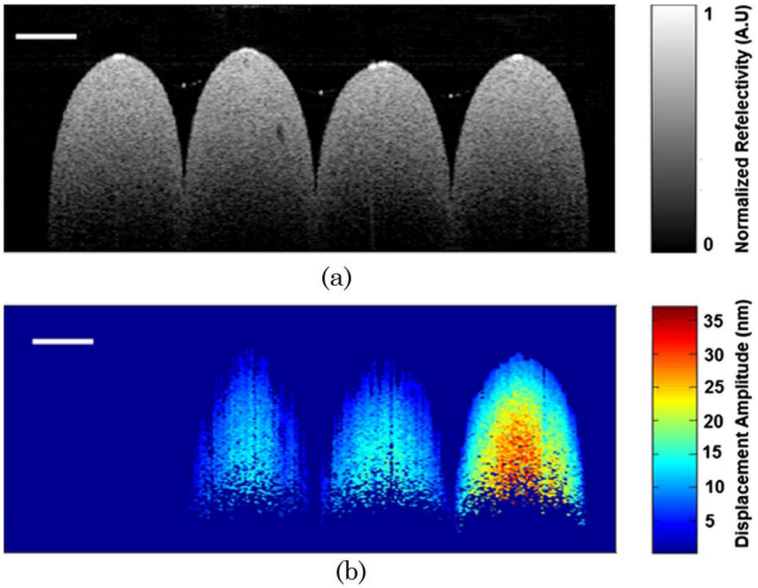

Fig. 3.

(Color online) (a) Conventional spectral domain structural OCT image of the tissue phantoms with four increasing nanoparticle concentrations of 0 mg/ml, 2.5 mg/ml, 5 mg/ml, and 10 mg/ml (from left to right). (b) PT-OCT image of the sample with ICG-encapsulated PLGA nanoparticle concentrations of 0 mg/ml, 2.5 mg/ml, 5 mg/ml, and 10 mg/ml (from left to right). The scale bar corresponds to 500 μm.